Progress In Electromagnetics Research M, Vol. 108, 187–200, 2022

A Novel Receiving Antenna Array Layout Method for Microwave Power Transmission

Jianxiong Li[1, 2, *] and Yuan Tan[1, 2]

Abstract—A novel layout method of receiving antenna array, which is a sparse random circular aperture array (SRCAA), to raise the power transmission efficiency (PTE) for microwave power transmission (MPT) is proposed in this paper. Different from the conventional antenna array layout, the array element positions of the SRCAA are randomly and uniformly distributed in the circular region. At present, the receiving array mostly adopts the form of uniform full array in the MPT system, and most researches focus on the antenna unit itself to raise the PTE rather than the array layout. In this paper, the initial array is obtained by randomly scattering points in the fixed area, and then the array element position is optimized by the algorithm to maximize the PTE between the transmitter (Tx) and receiver (Rx) of the MPT system. At the same time, the random array element position also plays a significant role in the uniformity of the received power of the receiving array. Therefore, this paper proposes a new index to measure the performance of the receiving array. In order to verify the effective performance of the SRCAA, we carried out a series of numerical simulations. Numerical simulation results show that the SRCAA, as a high-performance and low-cost receiving array, is more suitable for the receiving array of the MPT system than the traditional uniform array.

1. INTRODUCTION

Wireless power transmission technology includes electromagnetic induction, electric field coupling, electromagnetic resonance, microwave transmission, etc. The disadvantages of traditional wireless power transmission methods such as electromagnetic induction and magnetic coupling resonance are more and more obvious due to the limitation of transmission distance [1–3]. In contrast, microwave power transmission (MPT) technology has obvious advantages in distance. It means that power is loaded on the antenna and then transmitted to the specified position through microwave in free space. This is also the core technology of space solar power station (SSPS) [4, 5], and this technology breaks the distance limitation of traditional technology. When the MPT technology is successfully popularized and applied, we can really get rid of the shackles of cables.

For MPT system, the total efficiency is the product of several sub-efficiencies, including the conversion efficiency of the microwave generator, the transmission efficiency from the microwave source to the receiving antenna, and the rectification efficiency of the rectifier circuit at the receiving end [6, 7]. For the receiving antenna array, the main performance index is power transmission efficiency (PTE), which is defined as the ratio of the power received by the receiving array at the receiving end to the transmission power of the transmitting array at the transmitting end [8]. In order to obtain higher PTE, many studies have focused on the aperture illumination distribution of transmitting and receiving antennas [9–11]. The received power of the whole receiving array is obtained by calculating the radiation of a single transmitting array element and superimposing the power received by each receiving array

Received 9 December 2021, Accepted 8 February 2022, Scheduled 23 February 2022

* Corresponding author: Jianxiong Li (lijianxiong@tiangong.edu.cn).

[1] School of Electronic and Information Engineering, Tiangong University, Tianjin, China. [2] Tianjin Key Laboratory of Optoelectronic Detection Technology and Systems, Tianjin, China.

element, which is expressed in the form of finite series [12]. Through this calculation method, the accurate receiving power of the receiving array in the far-field region can be obtained. Rectenna array is generally divided into two parts: receiving antenna array and rectifier circuit. Then, according to the different power combination architecture, the form of rectenna array can be divided into three types [13]: (1) "architecture based on a single RF-to-DC converter": "the receiving antenna comprises an RF combining network which is responsible for the in-phase combination of the incoming waves", and then converting the RF waves to DC by using a single RF-to-DC converter. (2) "subarray-based arrangements": the overall receiving antennas are divided into subarrays "whose gathered signals are (locally) combined in RF and then converted to DC. Each subarray DC output is combined at the overall combiner, which is responsible for the power summation". (3) "combination of rectenna-collected signals at the DC level": "the straightforward combination at the DC of the signals received and converted by each antenna" [13]. According to [13], we can optimize the array element layout of the receiving array to obtain the maximum receiving power and then design the corresponding rectifier circuit. The design of rectifier circuit is a problem to be considered later, and this paper only considers the optimization of receiving antenna array. However, at present, there is no research mainly on the location layout of receiving antenna array elements, and most receiving arrays are uniform full arrays. Therefore, a new layout method is given in this paper. To the best of the knowledge of the authors, this is the first time to improve *PTE* by optimizing array element position. In this paper, a sparse random circular aperture array (SRCAA) is proposed. For the conventional concentric ring full array, its position is fixed, so the obtained *PTE* is also unchanged. Even after the array is thinly distributed, the array elements change their position along the ring or by changing the radius inward or outward through the ring, and the obtained *PTE* will not change greatly. On the contrary, the random array elements in the aperture can change their positions freely on the premise of meeting the minimum array element spacing, so it will cause great changes in *PTE*, and then higher *PTE* can be obtained through algorithm optimization. The array of [12] is optimized by the proposed method. The simulation results show that the *PTE* is improved by 4%, which proves the effectiveness of the proposed method. However, *PTE* also involves the beam collection efficiency (*BCE*) between the two arrays and the impedance matching between the array antenna and the free space [14–16]. In this paper, the transmitting array is fixed, and *BCE* calculates the power radiated into the receiving aperture. Therefore, when the transmitting array parameters and transmission distance are unchanged, *BCE* is unchanged, while this paper calculates the power received by the receiving array element, that is, the power obtained under this *BCE*. As for the impedance matching problem, we assume that the impedances of the array antenna and the free space in this paper are matched, so the calculation in this paper is also valid under this condition.

The main contributions of this paper are divided into the following points. Firstly, we propose a new receiving array model. Compared with the conventional uniform array, the SRCAA has the advantages of high efficiency, low cost, and simple structure. Secondly, we define a new index to measure the receiving performance of the receiving array. Finally, we conclude that the receiving array of the MPT system has a suitable scale. If it is smaller than this scale, the array efficiency will decline sharply. If it is larger than this scale, the array efficiency will not increase much, but will increase the system cost. In a word, the SRCAA is suitable for the receiving array of the MPT system.

2. MATHEMATICAL DERIVATION OF THE MAXIMUM *PTE* OF THE SRCAA

The system model of MPT is shown in Fig. 1. It is divided into a Tx array and an Rx array. The discussion is divided into three parts.

2.1. Transmitting Array

We set the Tx array as a uniform full array with fixed spacing between rings and between array elements on the ring. Assuming that the array aperture is D_t, the total number of array elements is N_T; C_t is the maximum number of rings; ρ_t is the radius of the t-th ring; N_t is the number of elements of the t-th ring;

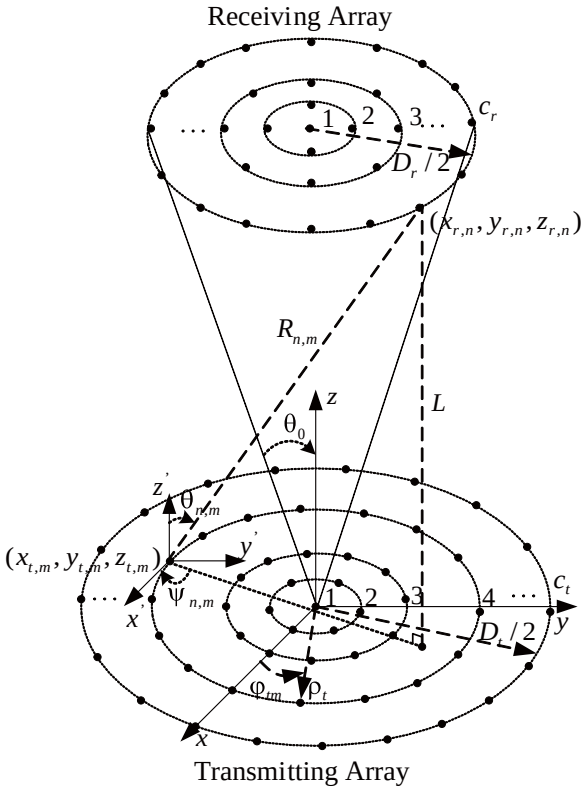

Figure 1. Geometry of the MPT system.

and φ_{tm} is the azimuth of the m-th element on the t-th ring. They satisfy the following conditions [17]:

$$\begin{cases} C_t = \left\lfloor \dfrac{D_t}{2d_{\min}} \right\rfloor \\ \rho_t = (t-1)d_{\min} \\ N_t = \left\lfloor \dfrac{4\pi\rho_t}{\lambda} \right\rfloor \\ \varphi_{tm} = \left\lfloor \dfrac{2\pi m}{\lambda} \right\rfloor \end{cases} \tag{1}$$

where $d_{\min}$ is the minimum array element spacing, λ the free space wavelength, and $\lfloor\cdot\rfloor$ a downward rounding function. Then the position coordinates of the m-th array element on the t-th ring are written as

$$\begin{cases} x_{t,m} = \rho_t \cos(\varphi_{tm}) \\ y_{t,m} = \rho_t \sin(\varphi_{tm}) \end{cases} \tag{2}$$

The Tx array and Rx array are in the same space rectangular coordinate system. The Tx array is in the XOY plane, and the coordinate position of the Tx element is $(x_{t,m}, y_{t,m}, z_{t,m})$, and $z_{t,m} = 0$. The excitation of the Tx element is obtained by Taylor synthesis method [18, 19]. For the Taylor array obtained by this method, the pattern is only close to the side lobe level in a region close to the main lobe, and then decreases monotonically, which makes the Tx array have good directivity. The Taylor distribution of circular aperture array is written as

$$g(p) = \sum_{n=0}^{\bar{n}-1} \frac{S(\gamma_{1n})}{J_0^2(\gamma_{1n}\pi)} J_0(\gamma_{1n}p), \quad p = \frac{\rho\pi}{a} \tag{3}$$

where a is the radius of array; $J_0(\cdot)$ corresponds to the zero-order Bessel function; $\bar{n}$ is the number of zeros; γ_{1n} is the zero of $J_1(\gamma_{1n}\pi)$; ρ is the radius of the ring; $S(\gamma_{1n})$ is the Taylor space factor of circular aperture array, which is written as

$$S(\gamma_{1n}) = \begin{cases} 1 & n = 0 \\ -J_0(\gamma_{1n}\pi)\dfrac{\prod\limits_{m=1}^{\bar{n}-1}\left[1-\left(\dfrac{\gamma_{1n}}{u_m}\right)^2\right]}{\prod\limits_{\substack{m=1 \\ n\neq m}}^{\bar{n}-1}\left[1-\left(\dfrac{\gamma_{1n}}{\gamma_{1m}}\right)^2\right]} & n = 1, 2, \ldots, \bar{n}-1 \end{cases} \tag{4}$$

where u_m is the zero of $S(\gamma_{1n})$, and written as

$$u_m = \begin{cases} \delta\sqrt{A^2 + (m-1/2)^2} & 1 \leq m \leq \bar{n} \\ \gamma_{1m} & m \geq \bar{n} \end{cases} \tag{5}$$

when $m = \bar{n}$, the lobe broadening factor δ is Eq. (6), and R_0 is the level ratio of main lobe to side lobe.

$$\delta = \frac{\gamma_{1\bar{n}}}{\sqrt{A^2 + (n-1/2)^2}}, \quad A = \frac{\operatorname{arccosh}(\mathrm{R}_0)}{\pi} \tag{6}$$

2.2. Receiving Array

The structure of the Rx array is very simple. The initial array is obtained by randomly and uniformly scattering points in the circular region with a given aperture of D_r. The total number of array elements is N_r, so the coordinate position of the n-th Rx element can be set as $(x_{r,n}, y_{r,n}, z_{r,n})$, where $x_{r,n}$ and $y_{r,n}$ are the random values in $[-D_r/2, D_r/2]$, $z_{r,n} = L$, and L is the distance between the Tx array and Rx array. Taking the minimum element spacing constraint into consideration, $x_{r,n}$ and $y_{r,n}$ must satisfy the following conditions:

$$\begin{cases} \sqrt{x_{r,i}^2 + y_{r,i}^2} \leq D_r/2 \\ \sqrt{(x_{r,i} - x_{r,j})^2 + (y_{r,i} - y_{r,j})^2} \geq d_{\min} \end{cases} \quad i, j = 1, 2, \ldots, N_r,\ i \neq j \tag{7}$$

The number of random and uniform scattering points in a fixed circular aperture is limited, where D_r and N_r satisfy the following conditions:

$$N_r = 2D_r(D_r + 1) \tag{8}$$

On the premise of little impact on PTE, we reduce some array elements, which is beneficial for saving the cost of the MPT system. The numerical simulation results show that the effect of sparse array is better than that of the conventional full array, and the effect of power homogenization of receiving array is also good.

2.3. Power Transmitting Efficiency

The array received power is given by the following formula [12]:

$$P_r = \left(\frac{\lambda}{4\pi}\right)^2 \sum_{n=1}^{N_r}\left|\sum_{m=1}^{N_T}\sqrt{p_{tm}G_{tm}(\theta_{n,m}, \psi_{n,m})G_{rn}(\theta_{n,m}, -\psi_{n,m})}\frac{e^{-j(kR_{n,m}-\beta_m)}}{R_{n,m}}\right|^2 \tag{9}$$

where $\theta_{n,m}$ and $\psi_{n,m}$ are the pitch angle and azimuth angle of the n-th Rx element relative to the m-th Tx element in the coordinate system $X'O'Y'$ with the m-th Tx element as the origin, respectively. $R_{n,m}$ is the relative distance between the n-th Rx element and the m-th Tx element, which is written as

$$R_{n,m} = \sqrt{(x_{r,n} - x_{t,m})^2 + (y_{r,n} - y_{t,m})^2 + (z_{r,n} - z_{t,m})^2} \tag{10}$$

where p_{tm} is the excitation of the m-th Tx element, k the wave-number, and β_m the excited phase of the m-th Tx element. $G_{tm}(\theta_{n,m}, \psi_{n,m})$ is the realized gain of the co-polarization of the m-th Tx element in the direction of the n-th Rx element, and $G_{rn}(\theta_{n,m}, -\psi_{n,m})$ is the realized gain of the co-polarization of the n-th Rx element in the direction of the m-th Tx element. The total transmitted power (P_t) radiated from the transmitting array is then $\sum_{m=1}^{N_T} p_{tm}$. Finally, the PTE of the Rx array is written as

$$PTE = \frac{P_r}{P_t} = \frac{\left(\frac{\lambda}{4\pi}\right)^2 \sum_{n=1}^{N_r} \left| \sum_{m=1}^{N_T} \sqrt{p_{tm} G_{tm}(\theta_{n,m}, \psi_{n,m}) G_{rn}(\theta_{n,m}, -\psi_{n,m})} \frac{e^{-j(kR_{n,m} - \beta_m)}}{R_{n,m}} \right|^2}{\sum_{m=1}^{N_T} p_{tm}} \tag{11}$$

When the Rx array is located in the far-field region of a single Tx array element, the receiving power can be calculated using Eq. (9), regardless of whether the Rx array is located in the far-field region of the Tx array. Assuming that the aperture of the transmitting array element is D_e, the transmission distance L can be obtained according to the far-field conditions [12]

$$L \geq 2D_e^2/\lambda \tag{12}$$

3. PROPOSED METHOD FOR OPTIMAL SYNTHESIS OF THE SRCAA

According to Eq. (9), it can be seen that the received power is very sensitive to the relative position of the two arrays. Assuming that there is no barrier between the Tx and Rx arrays and that the Tx array is fixed, the PTE depends on the relative position between the elements of the two arrays. Therefore, we only need to optimize the array position to maximize the PTE. The following optimization model is established as

$$\begin{cases} \text{find } [X, Y, Z] = [x_{r,1}, x_{r,2}, \ldots, x_{r,N_r}, y_{r,1}, y_{r,2}, \ldots, y_{r,N_r}, z_{r,1}, z_{r,2}, \ldots, z_{r,N_r}] \\ \text{maximize } PTE_{\max}([X, Y, Z]) \\ \text{subject } (a) \sqrt{x_{r,i}^2 + y_{r,i}^2} \leq D_r/2 \\ \qquad (b)\ \sqrt{(x_{r,i} - x_{r,j})^2 + (y_{r,i} - y_{r,j})^2} \geq d_{\min} \quad i, j = 1, 2, \ldots, N_r,\ i \neq j \\ \qquad (c)\ z_{r,i} = L, \quad i = 1, 2, \ldots, N_r \end{cases} \tag{13}$$

where $[X, Y, Z]$ is the optimization variable, and $PTE_{\max}$ is the maximum PTE of the SRCAA with random Rx element position. The aim of above optimization model is to find the optimal array positions $[X, Y, Z]$ to maximize $PTE_{\max}$ under constrains of (a) and (b) in Eq. (13). However, the above model is a three-dimensional optimization problem, which will inevitably bring some difficulties to the optimization process. Therefore, assuming that the Tx array and Rx array are in the same spatial rectangular coordinate system, the Tx array is located in the XOY plane; the Rx array is located in the positive direction of the z-axis; and the distance L between the two arrays is fixed. The above model can be simplified as

$$\begin{cases} \text{find } [X, Y] = [x_{r,1}, x_{r,2}, \ldots, x_{r,N_r}, y_{r,1}, y_{r,2}, \ldots, y_{r,N_r}] \\ \text{maximize } PTE_{\max}([X, Y]) \\ \text{subject } (a) \sqrt{x_{r,i}^2 + y_{r,i}^2} \leq D_r/2 \\ \qquad (b) \sqrt{(x_{r,i} - x_{r,j})^2 + (y_{r,i} - y_{r,j})^2} \geq d_{\min} \quad i, j = 1, 2, \ldots, N_r,\ i \neq j \end{cases} \tag{14}$$

In this model, the optimization variable is changed from $[X, Y, Z]$ to $[X, Y]$, which transforms a three-dimensional problem into a two-dimensional problem. The initial array element position coordinates obey uniform random distribution in the aperture. The initial array element position coordinates are uniformly and randomly distributed in the aperture. After position transformation, some array elements

will reduce the array element spacing or overflow the boundary. For the processing after each position transformation, we check the array elements one by one. The inspection standard is to satisfy the conditions (a) and (b) in Eq. (14). If the conditions are satisfied, they will be retained, otherwise will be discarded, then a new random array element satisfying the conditions is regenerated.

First, compared with the traditional circular aperture uniform full array, an array with sparse and random uniform distribution in the circular aperture is proposed in this paper. According to Eq. (9), a larger position change will cause a larger change in *PTE*. Therefore, the effect of the proposed array is better than that of the uniform full array. And the processing of this method in the optimization process is simpler than the traditional array, which only needs to satisfy two conditions. Secondly, on the other hand, reducing some array elements will help to reduce the cost of the MPT system, and the *PTE* will not be reduced too much. Thirdly, the receiving array does not require directivity like the Tx array. The Rx array requires the receiving power of each array element within the receiving aperture to be as uniform as possible, because the Rx element is connected with the rectifier circuit, the rectifier diode is the main device of the rectifier circuit, and the diode has a breakdown voltage. If the receiving power is too large, it will damage the diode. However, most of the received power of the uniform array is concentrated in the middle region and gradually decreases to the outer circumference. On the contrary, the random array proposed in this paper can greatly reduce this problem. The particle swarm optimization algorithm (PSO) is used in this paper. Particle swarm optimization is a very classic algorithm. Its excellent performance can help us find the global optimal solution.

To sum up, the advantages of the method proposed in this paper lie in the following three aspects. Firstly, compared with the traditional uniform array, the random array will obtain higher *PTE*. Secondly, the proposed model is a sparse random array, which can save some cost. Finally, the random array element position also has a good effect on the received power uniformity of the receiving array.

4. SIMULATION AND NUMERICAL RESULTS ANALYSIS

In this section, we will divide the numerical simulation into three aspects and analyze the results. Firstly, we optimize the array in [12] and analyze the corresponding numerical results to prove the effectiveness of the SRCAA, then we compare the effects of uniform array and the SRCAA. Secondly, we carry out numerical simulations under different parameters, including D_r and N_r, and analyze the numerical simulation results. Finally, we analyze the defined uniformity ξ under different array apertures. The CPU adopted for all simulations is Intel Core i7-4510U at 2.0 GHz with 8 GB RAM, and the numerical analysis software is MATLAB R2018a in this paper.

For a more comprehensive comparison, we introduce three evaluation indicators. The first is the sparse ratio χ, which is defined as the ratio of the number of array elements of the sparse array to the number of full array elements. The second is the received power uniformity ξ which is not defined in relevant literature. In this paper, it is temporarily defined as the ratio of the power density of the central region ψ in the receiving aperture to that of the whole receiving region. In this paper, the region accounting for one fourth of the receiving aperture radius is defined as the central region ψ, of course, the smaller the uniformity value, the better the array effect. The third is the sidelobe level of the receiving array *CSL* [20], which is defined as the ratio of the maximum power level outside the receiving area D_r to the maximum power level in the whole visible area Ω. The three indicators are defined as follows

$$\chi = \frac{N_{sparse}}{N_{full}} \tag{15}$$

$$\xi = \frac{P_{\psi}(\theta,\varphi)}{P_{D_r}(\theta,\varphi)} \tag{16}$$

$$CSL(\text{dB}) = 10\lg\frac{\max_{\theta,\varphi\notin D_r}|F(\theta,\varphi)|^2}{\max_{\theta,\varphi\in\Omega}|F(\theta,\varphi)|^2} \tag{17}$$

where $\psi \triangleq \{(\theta,\varphi) : 0 \le \theta \le \theta_\xi,\ 0 \le \varphi \le 2\pi\}$, $D_r \triangleq \{\theta,\varphi) : 0 \le \theta \le \theta_0,\ 0 \le \varphi \le 2\pi\}$, $\theta_\xi < \theta_0$ and $\Omega \triangleq \{(\theta,\varphi) : 0 \le \theta \le \pi,\ 0 \le \varphi \le 2\pi\}$. $F(\theta,\varphi)$ is the radiation pattern of array. θ_ξ is the pitch angle of the central region, and θ_0 is the pitch angle of the receiving aperture.

We optimize the array in [12]. In the original article, the Tx array is an 8×8 rectangular array, and the Rx array is a 2×2 array. Through numerical simulation, it is found that its PTE is 15.45%. Next, we keep the Tx array unchanged and change the Rx array to a circular array with an aperture of $D_r = 1.1\lambda$, and the number of array elements remains unchanged, but the array elements are randomly distributed in the aperture. After optimization, the PTE is 19.34%, an increase about 4%. After proving the effectiveness of the proposed method, we give the transmitting array as a uniform full array with aperture $D_t = 5\lambda$, so according to Eq. (1), $N_t = 93$ and $C_t = 5$. Because we mainly study the Rx array, in fact, the Tx array has nothing to do with our research goal, so we only set up one Tx array, and all numerical simulation results in this paper can be analogized to the case of different Tx arrays. In this paper, the frequency is 2.45 GHz, and L is 4λ. Fig. 2(a) shows the Tx elements positions and excitation obtained by applying Taylor weighting such that the side-lobe is less than -25 dB, and Fig. 2(b) is the corresponding radiation pattern.

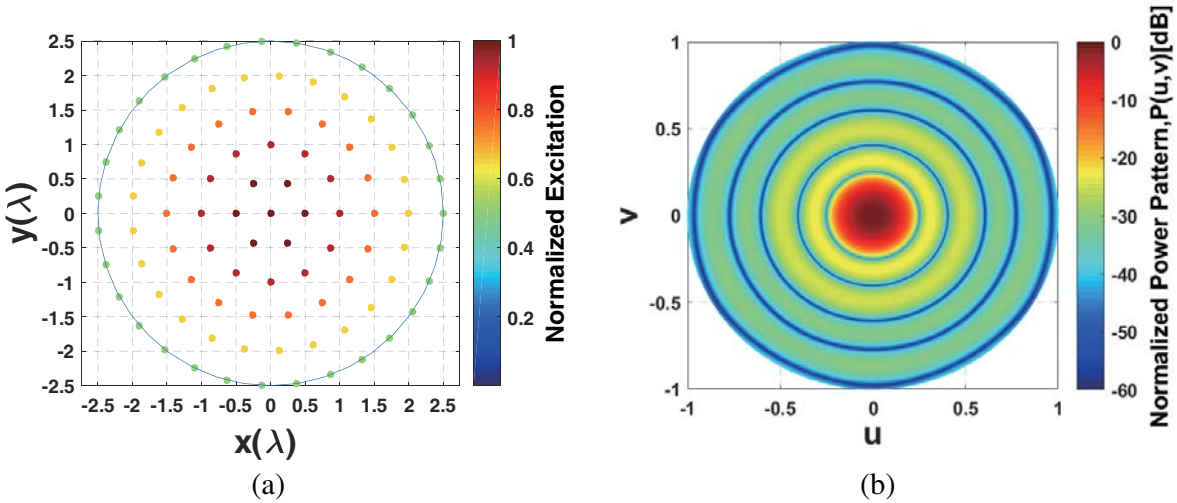

Figure 2. Synthesized results of the Tx array ($D_t = 5\lambda$ and $N_t = 93$) (a) layout and weight, (b) radiation power.

4.1. Comparison of Simulation Results between Uniform Array and SRCAA

Firstly, we let $D_r = 4\lambda$, and then compare its uniform array ($N_r = 52$) and sparse random array ($N_r = 35$). The results of uniform array are shown in Fig. 3 and sparse random array shown in Fig. 4.

Then, we let $D_r = 5\lambda$, and then compare its uniform array ($N_r = 63$) and sparse random array ($N_r = 56$). The results of uniform array are shown in Fig. 5 and sparse random array shown in Fig. 6.

The numerical simulation results are shown in Table 1. The result $[PTE, CSL, \chi, \xi]$ of $[D_r = 4\lambda, N_r = 52]$ is [33.1302, -19.05, 83.87, 12.32], and the result of $[D_r = 4\lambda, N_r = 35]$ is [37.9658, -16.89, 56.45, 4.12]. Compared with the uniform array, the array elements of the SRCAA are reduced by 17, and the PTE is increased by about 5%. However, the CSL is reduced by 3 dB, which is acceptable for the Rx array. In combination with Fig. 3 and Fig. 4, the uniformity of the SRCAA is much better than

Table 1. Synthesis numerical results of the SRCAA and uniform array.

$D_r(\lambda)$	N_r	PTE (%)	CSL (dB)	χ (%)	ξ (%)
4	52	33.1302	-19.05	83.87	12.32
	35	37.9658	-16.89	56.45	4.12
5	63	44.5022	-21.55	67.74	9.50
	56	43.4457	-19.92	55.92	5.08

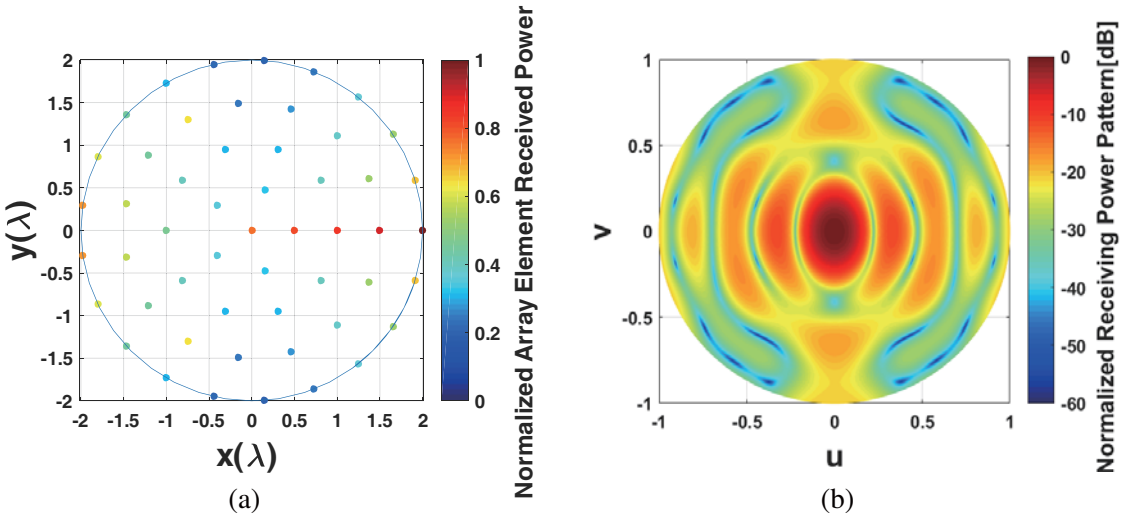

Figure 3. Synthesized results of the uniform Rx array ($D_r = 4\lambda$ and $N_r = 52$) (a) layout and received power, (b) receiving power.

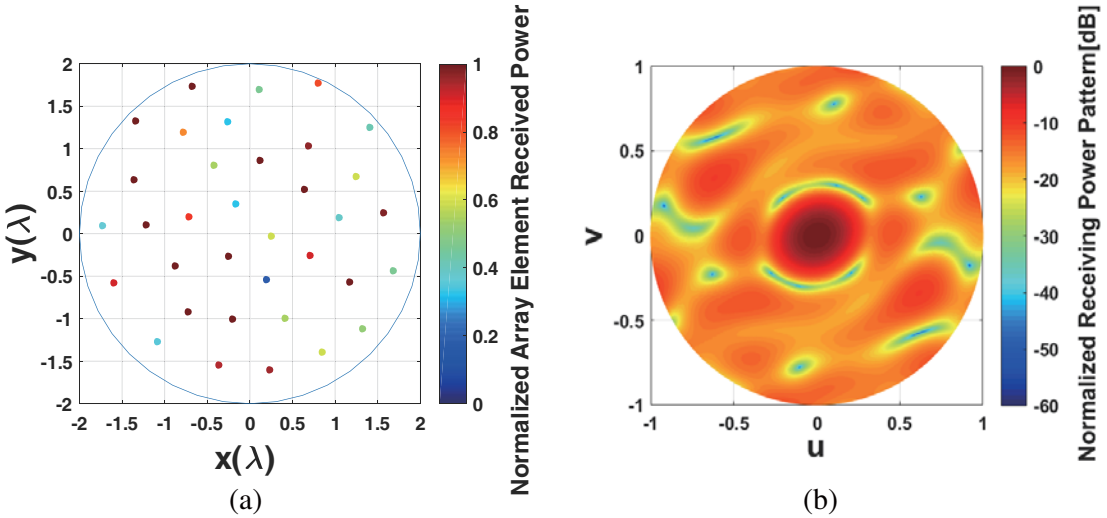

Figure 4. Synthesized results of the sparse random Rx array ($D_r = 4\lambda$ and $N_r = 35$) (a) layout and received power, (b) receiving power.

that of the uniform array, which can also be proved by the value of ξ, which is reduced by about 8%. According to the definition in Eq. (16), the smaller the ξ value is, the better, and the more uniform the received power of the array is. In addition, we also simulate the cases of [$D_r = 5\lambda$, $N_r = 63$] and [$D_r = 5\lambda$, $N_r = 56$], and the results are [44.5022, −21.55, 67.47, 9.50] and [43.4457, −19.92, 55.92, 5.08], respectively. However, after reducing 7 elements, the *PTE* is reduced by about 1%, the *CSL* is reduced by about 2 dB, and the uniformity is improved by about 4%, indicating that the value of *PTE* is also related to the array aperture N_r.

4.2. Effects of Different Parameters on Synthesized Results

In order to conduct a comprehensive and effective analysis, we conducted numerical simulations with several different parameters, and the results are shown in Table 2. In Table 2, the situations of [$D_r = 4\lambda$, $N_r = 52$] and [$D_r = 5\lambda$, $N_r = 63$] are uniform array, and the rest are sparse random arrays. From the analysis of Subsection 4.1, it is concluded that the performance of the SRCAA is better than that of

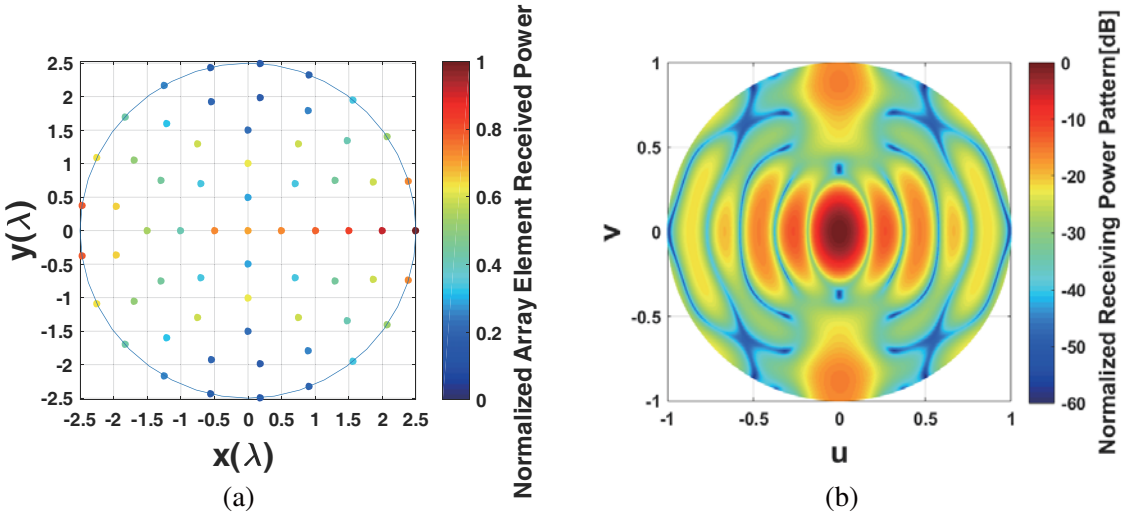

Figure 5. Synthesized results of the uniform Rx array ($D_r = 5\lambda$ and $N_r = 63$) (a) layout and received power, (b) receiving power.

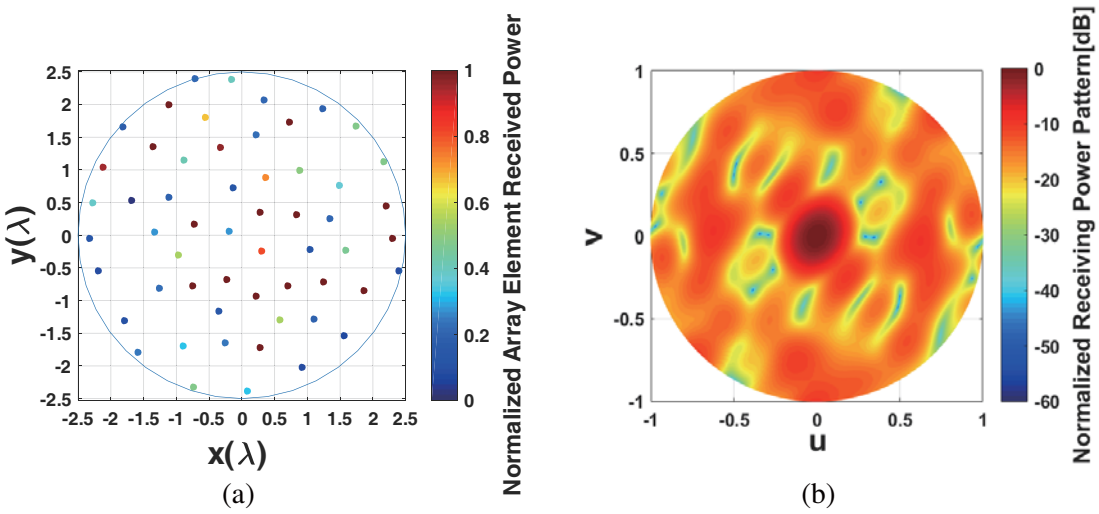

Figure 6. Synthesized results of the sparse random Rx array ($D_r = 5\lambda$ and $N_r = 56$) (a) layout and received power, (b) receiving power.

the traditional uniform array.

For the SRCAA, comparing the four cases [$D_r = 4\lambda$, $N_r = 40$], [$D_r = 4\lambda$, $N_r = 35$], [$D_r = 5\lambda$, $N_r = 56$], and [$D_r = 5\lambda$, $N_r = 40$], the results are [40.3652, −19.08, 64.52, 4.69], [37.9658, −16.89, 56.45, 4.12], [43.4457, −19.92, 55.92, 5.08], and [33.3595, −10.21, 43.01, 4.51], respectively. The array element position distribution and array received power are shown in Fig. 7, Fig. 4, Fig. 6, and Fig. 8, respectively. Through comparison, it can be concluded that when the aperture D_r remains unchanged, the more the number of array elements N_r is, the higher the *PTE* and *CSL* are; however, the uniformity will decrease, but not much. On the other hand, comparing [$D_r = 4\lambda$, $N_r = 40$] and [$D_r = 5\lambda$, $N_r = 40$], it is found that when N_r is constant, the larger D_r is, the *PTE*, *CSL*, and ξ will decrease, especially the *PTE* will decrease a lot.

When we continuously increase the array aperture D_r and the number of elements N_r, such as when $D_r = 10\lambda$, and $N_r = 180$, $N_r = 200$, respectively, the corresponding results are [49.1509, −11.83, 36.61, 14.62], [52.7052, −10.39, 38.68, 12.51], shown in Fig. 9 and Fig. 10. We find that even if the receiving array is large enough (twice as large as the transmitting array), there are enough elements,

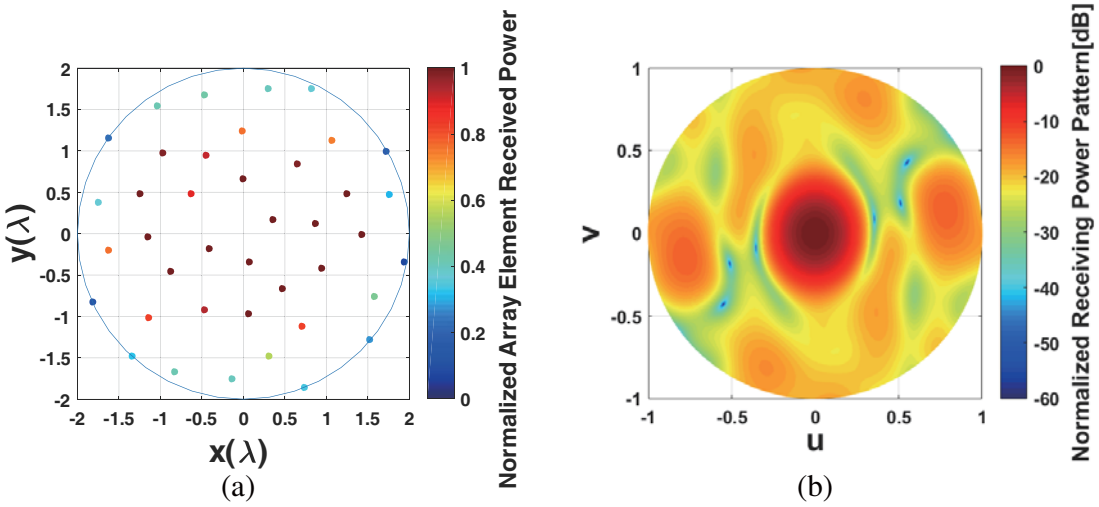

Figure 7. Synthesized results of the sparse random Rx array ($D_r = 4\lambda$ and $N_r = 40$) (a) layout and received power, (b) receiving power.

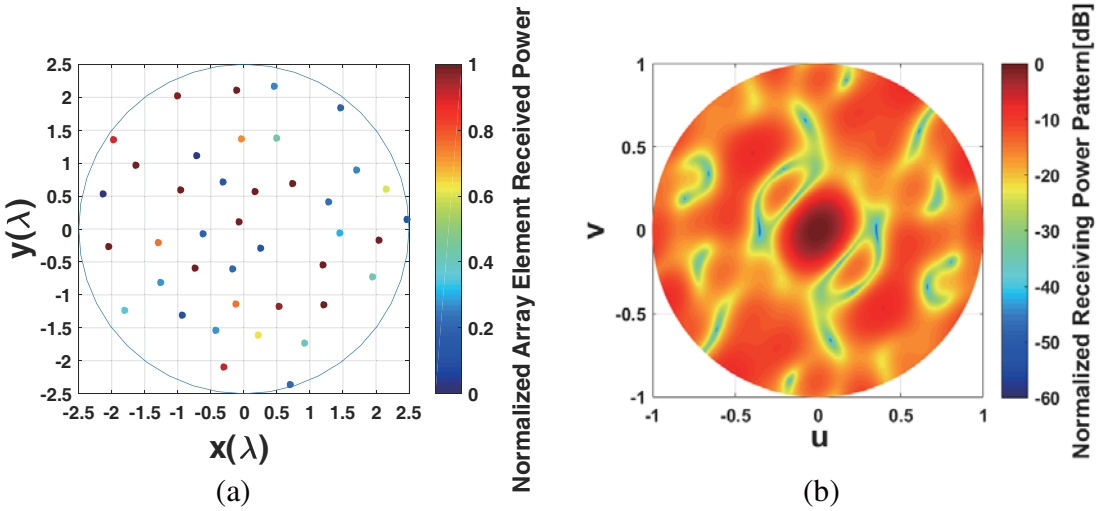

Figure 8. Synthesized results of the sparse random Rx array ($D_r = 5\lambda$ and $N_r = 40$) (a) layout and received power, (b) receiving power.

but the PTE does not improve much. This is because the power radiated into the receiving aperture is mainly divided into three parts:

$$P_R = P_{\sum} + P_L + P_I \tag{18}$$

where P_Σ is the reradiated power of the receiving antenna, P_L the power absorbed by the antenna load, and P_I the power loss of conductor and medium. It means that the maximum received power of the receiving array is certain and is affected by many factors [21]. All the power radiated to the receiving area is not completely absorbed by the receiving antenna, including those not radiated to the receiving surface of the antenna and reradiated by the antenna [22]. For these aspects, existing studies have also proposed corresponding solutions, such as super surface absorbing materials, making the array elements close as much as possible on the premise of meeting the minimum spacing of the array elements. In order to clarify the relationship between PTE and D_r, N_r, we conducted ten numerical simulations to continuously increase D_r and N_r. The result is shown in Fig. 11. It can be seen from the broken line diagram of their relationship that at the beginning, the PTE changes greatly with D_r and N_r, and in the later stage, this change becomes gentle. This also shows that for the receiving end, the receiving

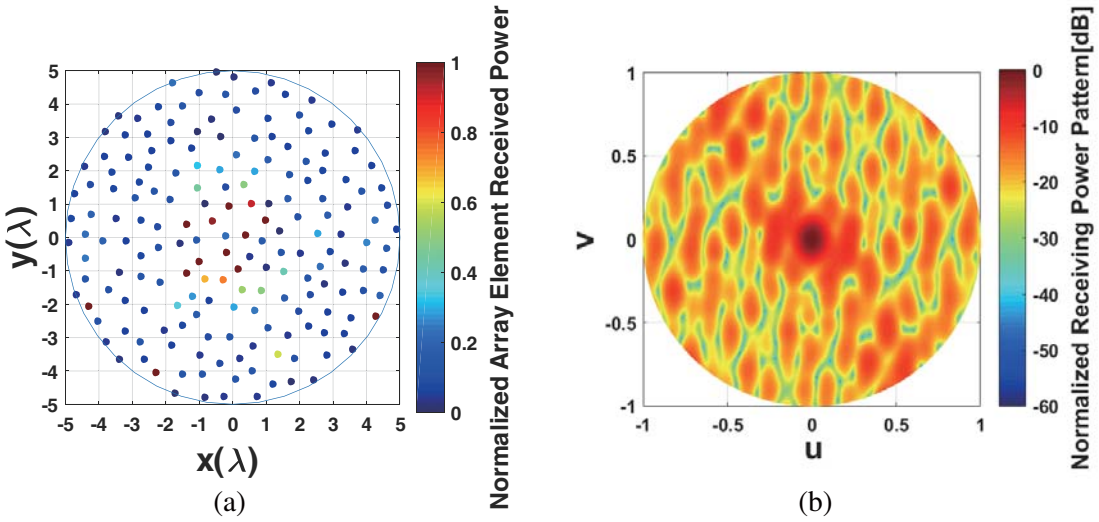

Figure 9. Synthesized results of the sparse random Rx array ($D_r = 10\lambda$ and $N_r = 180$) (a) layout and received power, (b) receiving power.

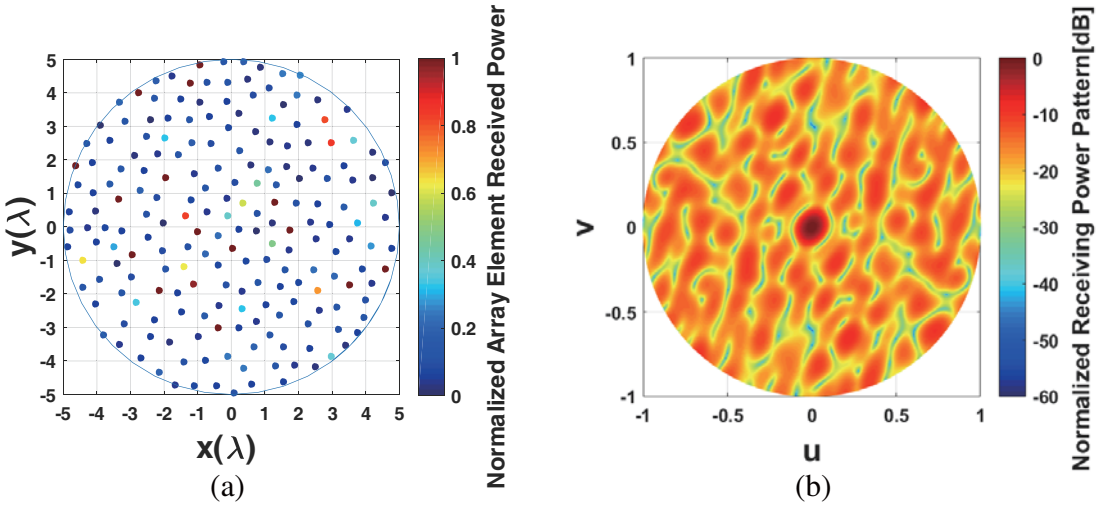

Figure 10. Synthesized results of the sparse random Rx array ($D_r = 10\lambda$ and $N_r = 200$) (a) layout and received power, (b) receiving power.

array has a suitable aperture, and if continue to expand this aperture, the *PTE* may not change much, but will cost more.

To sum up, we can conclude that the performance of the SRCAA is better than that of the traditional uniform array. It is known that the *PTE* of the receiving array mainly depends on two factors in the ideal state, the array aperture and the number of elements. When the array aperture is constant, the more the number of elements is, the higher the *PTE* is. On the contrary, when the number of elements is constant, the smaller the array aperture is, the higher the *PTE* is.

4.3. Effects of Different Parameters on ξ

In order to explore the relationship between the proposed index ξ and the array scale, we continuously increase D_r and N_r, record the change of ξ, and draw a broken line diagram as shown in Fig. 12, where ξ is the mean value during 100 iterations. We can see from the figure that with the continuous increase of D_r and N_r, ξ is also increasing, which means that the received power uniformity of the

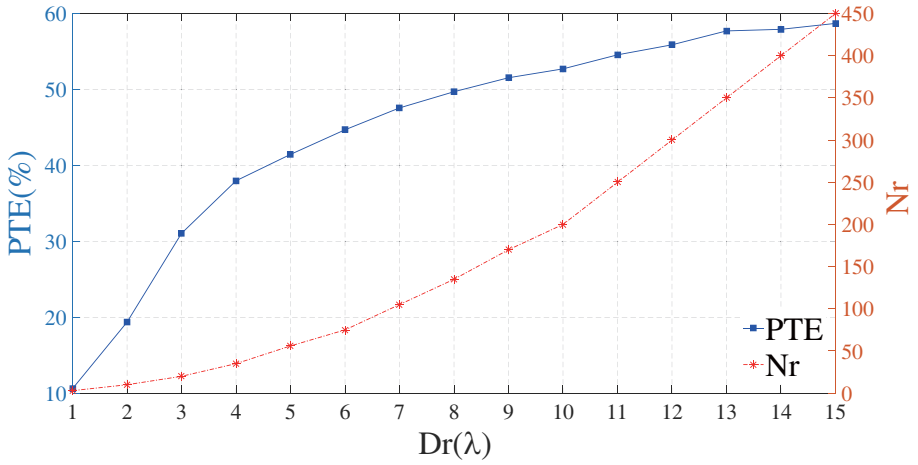

Figure 11. Behavior of *PTE* of the SRCAA versus the aperture D_r and the number of elements N_r.

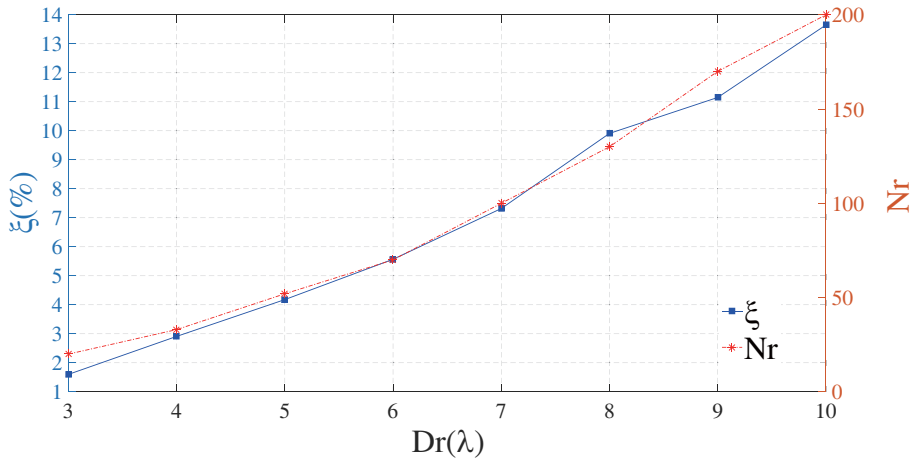

Figure 12. Behavior of ξ of the SRCAA versus the aperture D_r and the number of elements N_r.

Table 2. Synthesis numerical results of the SRCAA under different aperture size and elements number.

$D_r(\lambda)$	N_r	*PTE* (%)	*CSL* (dB)	χ (%)	ξ (%)
4	52	33.1302	−19.05	83.87	12.32
	40	40.3652	−19.08	64.52	4.69
	35	37.9658	−16.89	56.45	4.12
5	63	44.5022	−21.55	67.74	9.50
	56	43.4457	−19.92	55.92	5.08
	40	33.3595	−10.21	43.01	4.51
10	200	52.7052	−10.39	38.68	12.51
	180	49.1509	−11.83	36.61	14.62

array is decreasing. This is because the central area ψ defined by us is increasing, resulting in the increase of ξ. This also confirms what we mentioned above; for a fixed transmitting array, the receiving array has an appropriate scale, and exceeding this scale will not only slow the growth of *PTE*, but also increase the cost and even reduce the uniformity. In essence, the uniformity is mainly related to the

position distribution of the array elements, because the transmitting array is necessary to point the beam towards the receiving area, and the more concentrated the beam is, the better. This leads to the situation that the receiving power in the middle area of the traditional receiving array is too high, and that in other areas is too low, which brings great trouble to the subsequent rectifier circuit design. The proposal of the SRCAA greatly alleviates this situation, which also brings some references for the uniformity optimization of the receiving array.

5. CONCLUSION

In this paper, we propose a sparse random model of a circular aperture array, which is SRCAA, for the MPT system. Compared with the traditional uniform circular aperture array, the SRCAA has the advantages of simple structure, low cost, and remarkable effect. The SRCAA has no need to specially calculate the positions of the array elements, which are randomly generated under the conditions and uniformly distributed in the receiving aperture. The two conditions to be satisfied are that the distance between any two array elements in the aperture is greater than or equal to the minimum array element spacing. Therefore, its structure is very simple. After this structure is proposed, we only need to optimize the array element position by algorithm to obtain the optimal *PTE*. In addition, in order to measure the performance of the receiving array, we propose a new index, that is, the uniformity of the receiving power of the array. For the receiving array, uniformity is a very important index, and if the receiving power distribution is uneven, it will bring great trouble to the subsequent rectification.

In order to verify the performance of the SRCAA, we carried out a series of numerical simulations. Firstly, we use the proposed array model to optimize the array in [12]. The results show that the *PTE* is about 4% higher than the original. Next, we simulate the SRCAA under different parameters, including array aperture D_r and array element number N_r. The results show that under the condition of fixing one of the parameters, the *PTE* of SRCAA is directly proportional to N_r and inversely proportional to D_r. When the transmitting array remains unchanged, the receiving array has an appropriate scale. Beyond this scale, the growth of *PTE* will become very slow, but the cost will be greatly increased. Finally, we analyze the received power uniformity of the new index array proposed in this paper. It is concluded that the value of ξ mainly depends on the position distribution of the array elements, but for the same transmitting array, ξ will increase with the increase of the aperture of the receiving array.

In conclusion, a novel receiving antenna array (SRCAA) is proposed in this paper. Compared with the conventional uniform array, the SRCAA is more suitable for the MPT system. It can provide some reference for the specific practice of the MPT system.

ACKNOWLEDGMENT

This work was supported by the National Natural Science Foundation of China (Grant No. 51877151) and the Program for Innovative Research Team in University of Tianjin (Grant No. TD13-5040).

REFERENCES

1. Upasani, D. E., S. B. Shrote, and V. P. Wani, "Wireless electrical power transmission," *Int. J. Comput. Appl*, Vol. 1, No. 18, 6–10, 2010.
2. Shidujaman, M., H. Samani, and M. Arif, "Wireless power transmission trends," *International Conference on Informatics*, Dhaka, Bangladesh, March 2014.
3. Takeno, K. and Kazuhiko, "Wireless power transmission technology for mobile devices," *IEICE Electronics Express*, Vol. 10, No. 21, 1–11, 2013.
4. Matsumoto, H., "Space solar power station (SSPS) and microwave power transmission (MPT)," *IEEE Topical Conference on Wireless Communication Technology*, 6, Kyoto, Japan, November 2003.
5. Sasaki, S., K. Tanaka, and K. Maki, "Microwave power transmission technologies for solar power satellites," *Proceedings of the IEEE*, Vol. 101, No. 6, 1438–1447, 2013.

6. Qiang, C., C. Xing, and F. Pan, "A comparative study of space transmission efficiency for the microwave wireless power transmission," *2015 IEEE Asia-Pacific Microwave Conference (APMC)*, 1–3, Nanjing, China, December 2016.
7. Takahashi, T., T. Sasaki, Y. Homma, et al., "Phased array system for high efficiency and high accuracy microwave power transmission," *IEEE International Symposium on Phased Array Systems & Technology*, Waltham, MA, January 2017.
8. Brown, W. C. and E. E. Eves, "Beamed microwave power transmission and its application to space," *IEEE Transactions on Microwave Theory & Techniques*, Vol. 40, No. 6, 1239–1250, 1992.
9. Zhang, S., L. W. Song, B. Y. Duan, et al., "Aperture amplitude field integrated design of receiving and transmitting antenna for microwave power transmission," *IEEE Antennas and Wireless Propagation Letters*, Vol. 19, No. 7, 1216–1220, 2020.
10. Wan, S. and K. Huang, "Methods for improving the transmission-conversion efficiency from transmitting antenna to rectenna array in microwave power transmission," *IEEE Antennas and Wireless Propagation Letters*, Vol. 17, No. 4, 538–542, 2018.
11. Nepa, P. and A. Buffi, "Near-field-focused microwave antennas: Near-field shaping and implementation," *IEEE Antennas and Propagation Magazine*, Vol. 59, No. 3, 42–53, 2017.
12. Song, C. M., S. Trinh-Van, S. H. Yi, et al., "Analysis of received power in RF wireless power transfer system with array antennas," *IEEE Access*, Vol. 9, 76315–76324, 2021.
13. Massa, A., G. Oliveri, F. Viani, et al. "Array designs for long-distance wireless power transmission — State-of-the-art and innovative solutions," *Proceedings of the IEEE*, Vol. 101, No. 6, 1464–1481, 2013.
14. Diamond, B. L., "A generalized approach to the analysis of infinite planar array antennas," *Proceedings of IEEE*, Vol. 56, 1837–1851, 1968.
15. Stark, L., "Microwave theory of phased array antenna — A review," *Proceedings of IEEE*, Vol. 62, 1661–1701, 1974.
16. Shinohara, N., *Wireless Power Transfer via Radio waves*, ISTE Ltd. and John Wiley & Sons, Inc., 2014.
17. Li., J., J. Pan, and X. Li, "A novel synthesis method of sparse nonuniform-amplitude concentric ring arrays for microwave power transmission," *Progress In Electromagnetics Research C*, Vol. 107, 1–15, 2020.
18. Rahardjo, E. T., E. Sandi, and F. Y. Zulkifli, "Design of linear sparse array based on the Taylor line source distribution element spacing," *2017 IEEE Asia Pacific Microwave Conference (APMC)*, 61-64, Kuala Lumpur, Malaysia, November 2017.
19. Zinka, S, R. and J. P. Kim, "On the generalization of taylor and bayliss n-bar array distributions," *IEEE Transactions on Antennas and Propagation*, Vol. 60, No. 2, 1152–1157, 2011.
20. Oliveri, G., L. Poli, and A. Massa, "Maximum efficiency beam synthesis of radiating planar arrays for wireless power transmission," *IEEE Transactions on Antennas and Propagation*, Vol. 61, No. 5, 2490–2499, 2013.
21. Bui-Van, H., M. Arts, C. Craeye, et al., "On the maximum absorbed power in receiving antenna arrays," *IEEE Transactions on Antennas and Propagation*, Vol. 67, No. 3, 1993–1995, 2019.
22. Kojima, S., N. Shinohara, and T. Mitani, "Synthesis loss in receiving array antennas and transmission efficiency in the Fresnel region," *Wireless Power Transfer*, Vol. 4, No. 2, 120–131, 2017.